# Improvement of Negative Ion Source with Multi-Slot Grids for LHD-NBI

K. Tsumori 1), S. Asano 2), K. Nagaoka 1), M. Osakabe 1), K. Ikeda 1), Y. Takeiri 1), Y. Oka 1), O. Kaneko 1), Y. Suzuki 2), J. Watanabe 2), T. Okuyama 2), K. Ichihashi 2), M. Shibuya 1), T. Kawamoto 1), T. Kondo 1), M. Sato 1) and E. Asano 1).

1) National Institute for Fusion Science, 322-6 Oroshi Toki, Gifu, 509-5292 Japan.
2) Power and Industrial Systems R&D Center, Toshiba Corporation, 4-1 Ukishima-cho, Kawasaki-ku, Kawasaki 210-0862, Japan.

e-mail contact of main author: tsumori@nifs.ac.jp

**Abstract.** In this article, we describe injection results on a negative ion source newly designed for one of the neutral beam injectors (NBI) in large helical device (LHD). The ion source consists of an accelerator with a combination of steering grid (SG) and multi-slot grounded grid (MSGG), whose transparency is about twice as large as that of conventional multi-hole grounded grid (MHGG). Due to the high transparency, the MSGG reduces the heat load carried by beam was much reduced comparing to the load onto MHGG. The maximum injection power increased drastically up to 4.4 MW at the energy of 180 keV in 2002 fiscal. In the ion source consisting of accelerator with MSGG, degradation of injection power was observed above the energy of more than 160 keV. The degradation was considered caused by saturation of yield of hydrogen negative ion ($H^-$). In order to obtain further injection power, temperature of plasma grid rises up from 210 $^oC$ to 240 $^oC$, and the arc balance was adjusted after changing total number of filaments from twenty-four to twenty-six. The injection power, consequently, reached 5.7 MW at the energy of 186 keV after improving the $H^-$ yield. The maximum beam energy of 189 keV was obtained, and the power and pulse duration were 5.0 MW and 2 second at that time.

## 1. Introduction

Hydrogen negative ions have an advantage of higher neutral efficiency than protons in their energy range of more than 100keV [1], and negative-ion-based neutral beam injectors were built for the large scaled devices for nuclear fusion research [2,3]. In LHD, the experiments with neutral beams have been continued with two beam lines since 1998, and the third beam line has been added and injected beams since 2001. In case of LHD plasma, neutral injection is the most reliable heating method to improve the plasma parameters and to generate plasmas [4,5]. Enhancement of beam injection power was expected to improve the performance of LHD plasmas and to extend the boundary of experimental parameters. In order to improve plasma parameters, successive development of the ion sources has been carried out to improve beam injection power. The injection power and the energy were less than 4 MW and 170 keV for the pulse duration of 2 second after four-years improvements of the ion sources. The power, however, was limited by voltage breakdowns at beam accelerator of the ion source. In order to break through the power limit, newly designed beam accelerator has been developed and installed for the ion sources in one of beam lines for LHD since 2002. The new accelerator consisted of grounded grids with long slot-type apertures instead of conventional circular apertures. The ion sources with MSGG succeeded to increase injection energy and power, while adjustment to the ion source was not sufficient. Some improvements were needed to obtain more injection power. The guideline to improve the injection power can be separated into following three issues. The first is to increase the maximum beam energy, which is strongly concerned with performance of beam accelerator. The next is to enhance $H^-$ current, which relates to production rate of $H^-$ ions and uniformity of $H^-$ yield over whole beam extraction area. Although these issues link each other, we separate here to simplify the argument. The last is to improve the efficiency of neutral beam through beam injection port. In following sections, we report on the structures of ion source consisting of MSGG, on comparison of injection powers with use of accelerators with MHGG and MSGG, and on enhancement of $H^-$ current by adjusting temperature of plasma grid and plasma uniformity.

## 2. Negative Ion Source with Multi-Slot Grounded Grid

Details of negative ion source with multi-slot grounded grid are described in elsewhere [6]. Figures 1(a) and 1(b) shows schematic cross-sectional views of negative ion source for LHD-NBI beam line 1 (BL1). The ion source is separated into two parts of the arc chamber and beam accelerator at an electrode called plasma grid, which divides the arc plasma and beam regions. The arc chamber is characterized by multi-cusp source with external magnetic filter. The chamber has hexagonal cross-sections in the both long and short sides

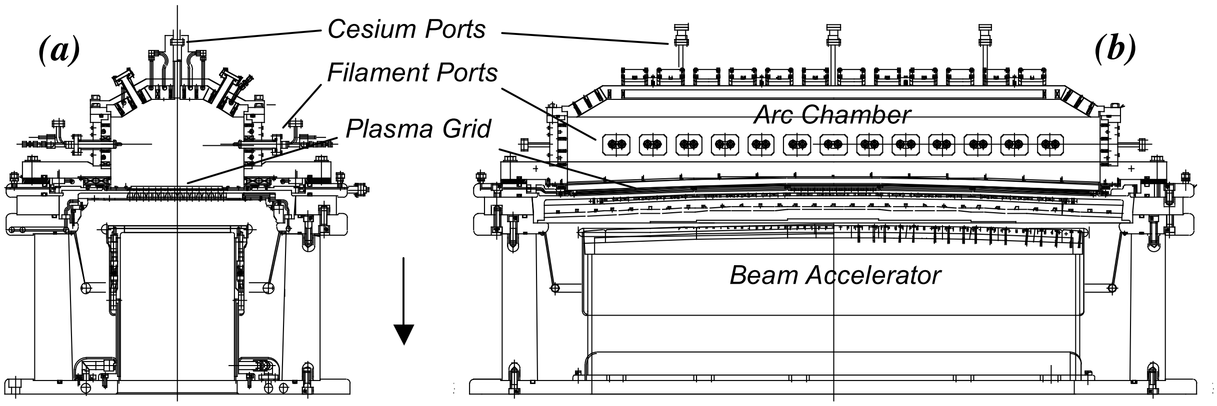


*FIG. 1(a) and 1(b). Cross-sectional views on the short side (a) and long side (b) of a negative ion source for one of LHD-NBIs (Beam line 1). The arrow indicates beam direction.*

to reduce magnetic lines of force connecting from filter magnet to cusp magnet and intersecting filaments. Those magnetic lines have a possibility to induce irregular arc discharge, which damages filaments and decreases the lifetime. Inner dimensions of the chamber are 1400 mm of the height, 350 mm of the width and 235 mm of the maximum depth. Cesium (Cs) vapor is seeded from three feeding lines equipped on the back plate to enhance the yield of hydrogen negative ions. Amount of Cs inside arc chamber is adjusted by remote-controlled pneumatic valves. Arc discharge is made by applying voltage of 40-80 V between arc chamber and filaments installed from side plates via filament ports. Thirty filament-ports are installed on each side of the chamber and twenty-four filaments are usually feed from filament power supply.

Beam accelerator is divided into five segments in long side direction of the ion source. The single segment is composed by four electrode grids, which are plasma grid (PG), extraction grid (EG), steering grid (SG) and multi-slot grounded grid (MSGG). The segments are inclined for extrapolation of the centerlines of these five segments to intersect at the pivot point 13 m apart from the exit plane of grounded grid. A cut view of the accelerator is illustrated in FIG. 2. Plasma grid is made of molybdenum to increase the temperature; i.e. appropriate PG temperature increases the $H^-$ ion yield in Cs seeded negative ion source. As shown in FIG. 2, permanent magnet array is embedded in EG, and polarities of the magnetic field are alternated row by row. The array magnets called electron deflection magnets (EDM), and local magnetic fields induced by the magnets sweep electrons extracted from arc chamber accompanying with $H^-$ ions. The grid is made of oxygen free copper (OFC) with water-cooling channels to keep temperature of EDM lower than the Curie point. The material of SG is molybdenum to prevent hard sputtering due to high-energy back-streaming positive ions coming from the beam downstream region. Multi-slot grounded grid is made of OFC, water channels are installed in the grid to remove heat carried by beams. A power supply is connected to PG and EG to extract $H^-$ ions from arc chamber. The $H^-$ ions are extracted from apertures of PG and the ions form multi-beamlets. The EG and SG have a common potential. Beamlets of $H^-$ ions passing through EG and SG are accelerated by potential difference between SG and MSGG.

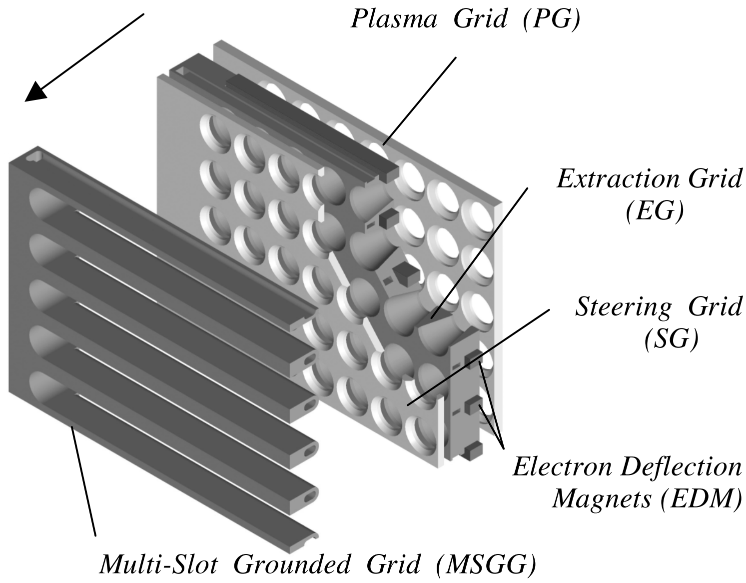


*FIG. 2. Cut view of accelerator segment with multi-slot grounded grid. The segment consists of four girds of PG, EG, SG and MSGG. The arrow indicates direction of $H^-$ beam.*

Each electrode segment performs to $H^-$ beamlets following three roles. The first role is beam focusing, which is defined by applied voltages to the grids and geometric structures of all the grids are defined. The second is beam converging. Each beamlets is converged at the pivot point by beam steering technique. Beamlets are steered by displacing the aperture axes of segment grids. The last is correction of beam trajectories deflected by EDM. The correction is also done by aperture displacement. In regard to BL1 of LHD-NBI, all the beamlet-axes are designed to intersect at the pivot point by beam focusing, converging and trajectory correction. Aperture axes in PG and EG are common and aperture of grounded grid (GG) were displaced in previous accelerator with MHGG. The maximum displacement of MHGG apertures became more then 3 mm. Accelerator with MSGG cannot steer any beamlet in the direction of slot long side, and SG is added to control beamlet trajectories. The maximum displacement of the SG aperture is smaller than 2 mm, and this has an advantage from the point of view of beam aberration comparing to GG steering system.

## 3. Comparison of Injection Power and Energy in Accelerators with MHGG and MSGG

The largest difference between $H^-$ and positive-ion accelerations is electron detachment by collisions of $H^-$ ions with neutral hydrogen molecules. The collision occurs during the transport of $H^-$ beam inside accelerator grids. Detached electrons, which are called stripped electrons, are independently accelerated from the collision points and are bent by magnetic field leaked from arc chamber. The stripped electrons scatter widely onto accelerator grids because of the randomness of the collision points in beam accelerating region and small Lamour radius of electrons. Acceleration voltage is higher than extraction voltage, and GG is exposed larger heat load carried by the stripped electrons. Neutralized hydrogen atoms and off-focus $H^-$ ions carry heat load additionally. The neutralization process of $H^-$ ions inside beam acceleration region is inevitable, because it is impossible to remove neutral gasses from the region. Energetic particles onto GG can cause gas emission and secondary ions emission via sputtering processes from the grid, and those emitted secondary particles can induce voltage breakdowns at the grid gap. One of the methods to reduce total heat load is to increase the beam transparency of GG. For this purpose, MSGG has been newly designed and replaced from previous MHGG. The beam transparency of MSGG is about twice as large as that of MHGG.

Figure 4 indicates Injection powers in both cases of accelerators with MHGG and MSGG. The data is plotted as a function of beam energy. The maximum injection power and energy are 3.6 MW and 165 keV for 2 second in pervious ion source with MHGG in LHD-NBI BL1. These values increased up to 4.4 MW and 180 keV by adopting MSGG to the accelerator. It took shorter time to reach the maximum power and energy in the accelerator equipping MSGG compared with MHGG. Main cause for shortening the attainable time was drastic decrease of breakdowns between accelerator grids, which is related to the reduction of heat load onto GG. Beam heat onto MHGG and MSGG was compared with the same beam condition by means of water-calorimetric measurement, and heat reduction rate was about 45 % in MSGG case. The reduction ratio is close to the ratio of beam interfarring area of GG [6]. Constitution of heat load due to

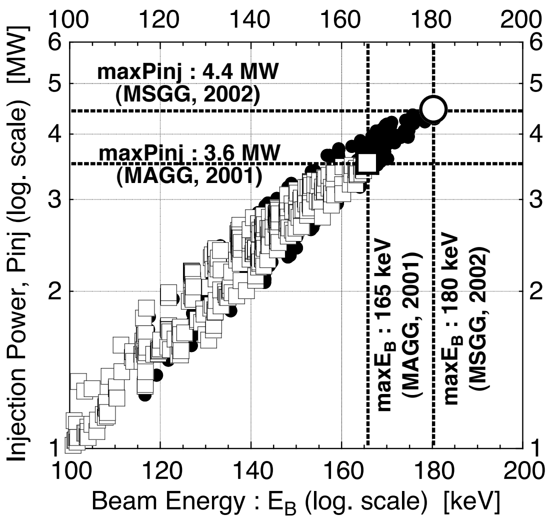


*FIG. 4. Comparison of injection power with respect to beam energy. The power is summation of two ion sources. Solid circles and open squares indicate injection powers in the cases of accelerators with MSGG and MHGG, respectively.*

stripped electron is considered not so large in total heat load to grounded grid, and the rest particles, neutralized $H^0$ and $H^-$ beam with strong aberration might deposit unexpected high heat load to GG.

## 4. Enhancement of $H^-$ Current

### 4.1 Saturation of $H^-$ Current

According to Child-Langmuir's low, injection power is approximately proportional to the 5/2 power of beam energy ($E_B$) under the condition that beam perviance, grid gaps and the ratio of *Vext / Vacc* (*Rv*) are kept constant. Where the notations of *Vext* and *Vacc* represent extraction and acceleration voltages, respectively, and beam energy is expressed as summation of these voltages. Injection power obtained by accelerator with MSGG is indicated with respect to beam energy in FIG. 5. Neutral beam line for LHD consists of two ion sources and injection power indicates summation of the powers obtained by those two ion sources here. Keeping beam energy constant, $H^-$ current goes up linearly as increasing input arc power, and then reaches to the maximum value corresponding to the space charge limited current at that energy. The lines A and B are drawn to cross the limited powers. As indicated in the figure, injection power changes the raising rate from line A to B at about the energy of 160 keV. The line A is proportional to $E_B^{5/2}$, while line B changes linearly with respect to $E_B$. This suggests the $H^-$ current saturates approximately in the energy above 160 keV. Following possibilities were expected in this situation. The first was mismatching of Cs condition for $H^-$ production, and the next was caused by imbalanced distribution of arc plasma and the last was insufficiency of input power to generate the seeds of $H^-$ ions; i.e. hydrogenous positive ions. The first and second were focused, because total $H^-$ current did not change by increasing input arc power.

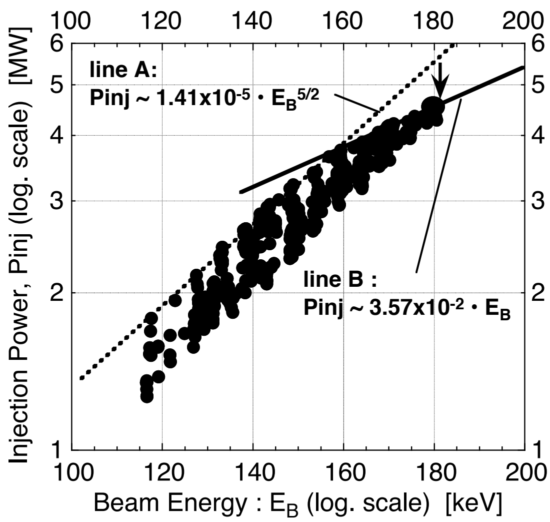


*FIG. 5. Injection power with respect to beam energy. The power is summation of two ion sources consisting of accelerators with MSGG. The lines A and B are proportional to the 5/2 power of beam energy ($E_B^{5/2}$) and to $E_B$, respectively.*

### 4.2 Enhancement of Cesium Effect

Assuming $H^-$ ions are dominantly produced via surface process in Cs seeded ion sources, workfunction of PG surface should have strong influence to the production rate of $H^-$ ions. In well-defined clean surface under ultra high vacuum condition, workfunction becomes minimum when Cs coverage is half monolayer [7]. In practical surface, such as PG surface of Cs seeded ion source, it is difficult to maintain the situation as static condition, because cesiated surface is exposed hydrogenous ions, electrons and other impurities. Nevertheless such violent situation of ion source, $H^-$ production rate does not change so much once Cs is injected a certain amount inside the arc chamber. Although small amount of Cs vapor should be supplied to the chamber, $H^-$ production rate becomes more sensitive to PG temperature. The PG temperature is risen by radiation from arc plasma and heat transfer of charged particles. Duty cycle of arc discharge is small, about 6 %, and thermal insulator is inserted between PG and PG retainer not to decrease the temperature quickly. Typical sensitivity of $H^-$ production rate to PG temperature is shown in FIG. 6. The temperature is measured at a PG periphery without aperture holes. In this figure $H^-$ current is normalized by the value at PG temperature of 210 $^oC$. Averaged PG temperature was about 210 $^oC$ in beam injection of 2002 fiscal. Production rate of $H^-$ ions still increases at PG temperature more than 210 $^oC$ as shown in FIG. 6. There are two ways to raise the temperature. One is to increase input arc power, which is a heat source. Anther is to decrease heat transfer from PG via thermal insulator. Arc power was limited by arcing, irregular arc discharge, and it was impossible to increase the arc power. The latter, therefore, was chose to enhance $H^-$ production rate.

By changing the material of thermal insulator of PG from OFC to stainless steal and decreasing the contact area, PG temperature can keep much higher than previous condition.

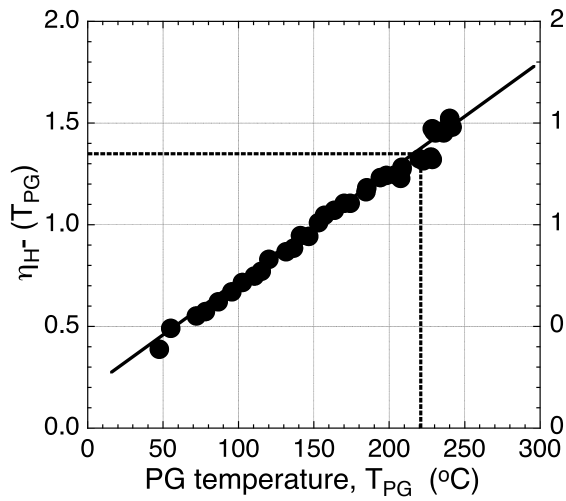


*FIG. 6. Production rate of $H^-$ ions as a function of temperature of plasma gird. The rate is normalized by the value of $H^-$ current at 210 $^oC$. The rate changes linearly to PG temperature in this temperature range.*

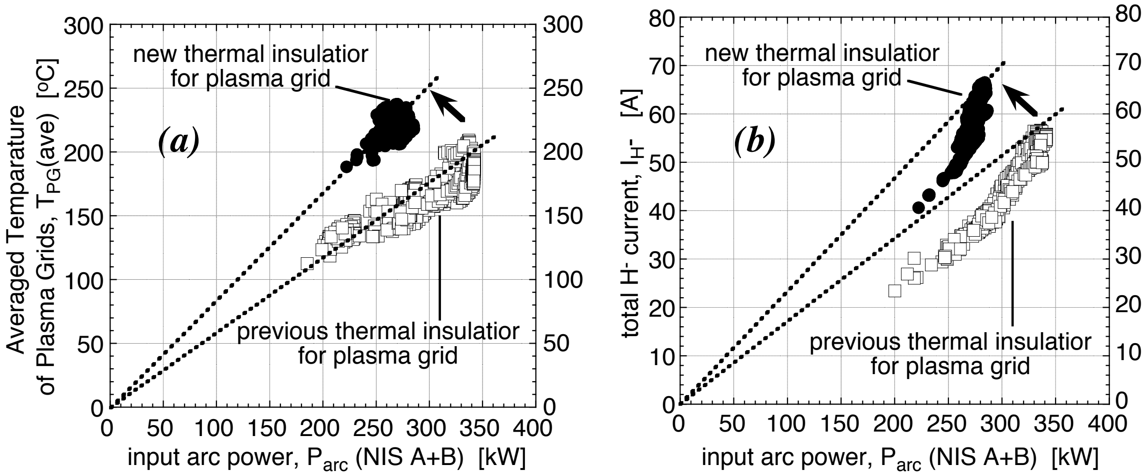


*FIG. 7(a) and 7(b) (a) Averaged temperature of plasma grids over two sources is shown as a function of arc power input to two ion sources. (b) Arc efficiency of $H^-$ current with respect to arc power. Solid circle and open square denote the data obtained by using new and old thermal insulators, respectively.*

Figure 7a shows averaged temperature of ten plasma girds, which corresponds to whole plasma electrodes of two ion sources, as a function of input arc power. The ratio of PG temperature to input arc power increased from 0.6 to 0.8 $^{o}C$ / kW. The maximum averaged PG temperature of 240 $^{o}C$ was obtained at arc power of about 120 kW per ion source. Arc efficiency, which is defined as total $H^-$ current to input arc power, enhanced after changing the thermal insulator. Larger current is obtained at lower arc power as shown in FIG. 7b. The efficiency changes from 0.172 to 0.235 [A/kW] at maximum. The higher efficiency of $H^-$ production rate to input arc power contributes to decrease irregular discharge of arc chamber and to save the filament lifetime.

### 4.3 Improvement for Arc Distribution

The short and long inner sides of arc chamber for LHD negative ion source are 350 mm and 14000 mm, respectively. Imbalance of arc-plasma distribution is observed in such elongated ion sources. Uniform distribution of arc plasma is effective to obtain large $H^-$ current and to avoid voltage breakdowns in accelerator due to spatial difference of beam perviance. Twenty-six filaments are prepared for each arc chamber of LHD-NBI BL1; thirty filaments are installed on each long sidewall of the chamber. Usually twenty-four filaments are feed from twelve-filament power supply (PS). All the filaments were feed to obtain symmetric and uniform distribution of filament arrangement in long side of the arc chamber. Additionally, plasma distribution was adjusted by using external resisters connected between filament and arc power supplies. Injection power after adjustments for PG temperature and plasma uniformity is shown in FIG. 8. Injection result before the adjustments is indicated in the same figure for comparison. Degradation of injection power due to saturation of $H^-$ current is shown as line A, and the feature is improved after the adjustments enhancing $H^-$ current. As indicated in FIG. 8, power degradation is removed after the adjustments, and injection power reaches 5.7 MW at the beam energy of 186 keV. The beam duration was 1.6 second, and the duration is limited by experimental requirement. The injection power becomes proportional to $E_B$ above the energy of 175 keV. In this energy range, drain current of acceleration PS, whose current includes about 75 % of $H^-$ current, is limited by capacitance of the PS. High-energy limit has been examined using the accelerator with MSGG. So far, the maximum energy was limited 189 keV by the voltage limit of acceleration PS, the injection power and pulse duration were 5.0 MW and 2 seconds, respectively.

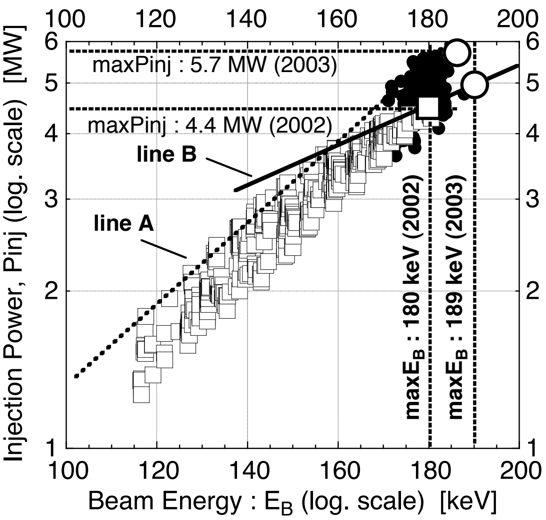


*FIG. 8 Beam injection power before and after adjustments for PG temperature and for uniformity of arc plasma.*

## 5. Summary

Beam accelerator with a combination of steering grid and multi-slot grounded grid was developed and applied to large scaled negative ion sources for LHD-NBI. Beam injection power increased from 3.6 MW to 4.4 MW by introducing the accelerator system in 2002 fiscal. The beam energy reached 180 keV, which is the design value of LHD-NBI. Although the beam energy attained the maximum value of power supply, injection power started to saturate above the energy of 160 keV. According to Child-Langmuir's low, injection power should be proportional to the 5/2 power of beam energy with some assumptions, while the power is linear to beam energy. This suggests the $H^-$ yield is not sufficient to input arc power. In order to increase the beam power, two-steps adjustment has been applied for enhancement of the $H^-$ current. The first one is to enhance cesium effect by rising averaged temperature of plasma grids from 210 $^oC$ to 240 $^oC$. The saturation characteristic has been disappeared by this adjustment of PG temperature. Another is to adjust the uniformity of arc plasma by adding total number of filaments in arc chamber. The injection power, consequently, attained the maximum value of 5.7 MW at the energy of 186 keV and the pulse duration was 1.6 second. Both of the beam power and energy exceed the design value of LHD-NBI. The maximum beam energy of 189 keV, which was limited by capacity of acceleration power supply, was obtained at the power of 5.0 MW so far.

## References

[1] BERKNER, K.H., et al., "Intense, Mixed-Energy Hydrogen Beams for CTR Injection", Nucl. Fusion, **15** (1975) 249-254.

[2] USHIGUSA, K., and the JT-60 TEAM, Proceedings of 16th IAEA Fusion Energy Conference, Montreal, Canada, 1996, (unpublished), IAEA-CN-64/01-3.

[3] MOTOJIMA, O., et al., "Initial physics achievements of large helical device experiments", Physics of Plasma **6** (1999) 1843-1850.

[4] TAKEIRI, Y.,et al., "Formation of electron internal transport barrier and achievement of high ion temperature in Large Helical Device", Phys. of Plasma, **10** No.5 (2003) 1788-1795.

[5] KANEKO, O., et al., "Analysis of plasma initiation by neutral beams in the Large Helical Device", Nucl. Fusion, **42** No.4 (2002) 441-447.

[6] TSUMORI, K., et al., "High power beam injection using an improved negative ion source for the large helical device", Rev. of Sci. Instrum, **75** No.5 (2004) 1847-1850.

[7] KIEJNA, A., and WOJCIECHOWSKI, K. F., "Work function of metals: Relation between theory and experiment", Prog. Surf. Sci, 11, (1981) 293-338.